Supplementary Information

I. CODE

All code used to produce figures in the main document, as well as all the figures in the present document are available at https://github.com/Bargo727/CellAlignment

Corresponding videos can also be found in the same repository.

II. CLOSURE OF THE MASTER EQUATION, AND DERIVATION OF THE MEAN-FIELD MODEL

As noted in the main document, Eq. (2) governing the evolution of occupation probabilities is not closed. Therefore, the complete master equation (ME) would include an infinite hierarchy of equations describing the evolution of all moments. To close the system at first order, we assume that neighboring sites on the lattices are uncorrelated, that is

$$p(n_{ij} = 1, n_{kl} = 1) = p_{ij}p_{kl}. \tag{S1}$$

This yields

$$\frac{dp_{ij}}{dt} = v_\kappa^+(i-1)p_{(i-1)j}(1-p_{ij}) + v_\kappa^-(i+1)p_{(i+1)j}(1-p_{ij})$$

$$- h_\kappa^+(j-1)(1-p_{i(j-1)})p_{ij} - h_\kappa^-(j+1)(1-p_{i(j-1)})p_{ij}. \tag{S2}$$

We have verified numerically that Eq. (S1) holds approximately for a range of trap sizes and growth rate kernels (see Fig. S3).

We can use Eq. (S2) to obtain a mean field approximation of the model. This amounts to averaging growth rates over the spatial domain. Let

$$\bar{v} \equiv \frac{1}{M}\sum_{i=1}^{M} v_\kappa^+(i), \qquad \bar{h} \equiv \frac{1}{N}\sum_{j=1}^{N} h_\kappa^+(j), \qquad n \equiv \frac{1}{MN}\sum_{i,j} p_{ij}. \tag{S3}$$

The first step in obtaining the mean field is to replace the space-dependent rates in Eq. (S2) with Eq. (S3). The SMM model can then be approximated by

$$\frac{dp_{ij}}{dt} = 2\bar{v}n(1-p_{ij}) - 2\bar{h}(1-n)p_{ij}, \tag{S4}$$

with the appropriate adjustment of the coefficients for the equations for the boundary sites. Summing over all lattice sites yields

$$MN\frac{dn}{dt} = 2MN\bar{v}n(1-n) - 2N\bar{v}n(1-n) - 2MN\bar{h}n(1-n) + 2M\bar{v}n(1-n),$$

with the second and fourth terms coming as a result of the SMM equations on the boundary of the lattice. Dividing through by MN yields the logistic equation,

$$\frac{dn}{dt} = 2\Big(\bar{v}\Big(1-\frac{1}{M}\Big) - \bar{h}\Big(1-\frac{1}{N}\Big)\Big)n(1-n) \equiv \mu(\kappa, M, N)n(1-n). \tag{S5}$$

We can solve Eq. (S5) with initial condition $n(0) = \frac{1}{2}$ since initial cell orientations are random, and the fraction of vertical cells is initially half. We obtain,

$$n(t) = \frac{Ce^{\mu(\kappa,M,N)t}}{Ce^{\mu(\kappa,M,N)t}+1}.$$

Setting $C = 1$ satisfies the initial condition.

III. RELATIONSHIP BETWEEN κ^* AND s

We next derive the relationship between κ^* and the scaling parameter s. Recall that the size of the trap for fixed M and N is defined to be $sM \times sN$.

For exponential kernels,

$$\bar{v} = \frac{\lambda}{sM}\Big(\frac{1-e^{-sM\kappa}}{1-e^{-\kappa}}\Big) \qquad \bar{h} = \frac{\lambda}{sN}\Big(\frac{1-e^{-sN\kappa}}{1-e^{-\kappa}}\Big)$$

We set the growth term in Eq. (S5) equal to 0. Motivated by our numerical observation that κ^* is small, we expand the resulting equation to $O(\kappa^2)$ and obtain

$$\frac{1}{sM}\Big(sM\kappa - \frac{(sM\kappa)^2}{2}\Big)\Big(1-\frac{1}{sM}\Big) - \frac{1}{sN}\Big(sN\kappa - \frac{(sN\kappa)^2}{2}\Big)\Big(1-\frac{1}{sN}\Big) = 0.$$

Simplifying gives

$$\kappa\Big(\frac{s(N-M)}{2}\Big) = \frac{N-M}{sMN},$$

which yields

$$\kappa^* = \frac{2}{MNs^2}.$$

The same approach works for kernels of the form

$$v_\kappa^+(i) = \frac{\lambda}{1+\kappa(sM-i)^\alpha}, \qquad \alpha \in (0,\infty).$$

We have

$$\sum_{i=1}^{sM} v_\kappa^+(i) \approx \int_1^{sM} v_\kappa^+(x)dx,$$

where $v_\kappa^+(x)$ is the continuous analog of the growth rate $v_\kappa^+(i)$. For small κ, we have

$$\int_1^{sM} v_\kappa^+(x)dx \approx sM - \frac{\kappa(sM)^{\alpha+1}}{\alpha+1} \tag{S6}$$

Substituting Eq. (S6) and the corresponding result for $\bar{h}$ into Eq. (S5) and setting the growth rate equal to 0 yields, for large s,

$$\kappa^* = \frac{(\alpha+1)(N-M)}{MNs^{\alpha+1}(N^\alpha - M^\alpha)}$$

IV. MODEL WITH LONG-RANGE INTERACTIONS

As noted in the main text, a spatial Moran model (SMM) that incorporates long-range interactions produces behavior similar to the SMM. In this model, growth rates are defined and modified as described in the main text. However, the *effect* of cellular division induces long-range changes. In the SMM described in the main text, if a vertical cell divides at the ij-th site divides, it will replace a cell at site $(i \pm 1)j$ with a copy of itself.

On the other hand, in a model with long-range interactions, a vertical cell dividing at the ij-th site will place a copy of itself at site $(i \pm 1)j$ and then displace all other cells between it and the boundary in the direction of its growth by one spatial unit. That is, if growth is in the + direction, the the cell at site $(i+k)j, 1 \leq k \leq M-i$ will move to site $(i+k+1)j$, and the boundary cell at location Mj is removed from the system (pushed out of the trap). See Fig. S6 for examples of how this model approaches equilibrium from a random initial condition. This long-range model was also implemented using the Gillespie algorithm, and is available in the repository mentioned above.

V. SUPPLEMENTARY FIGURES

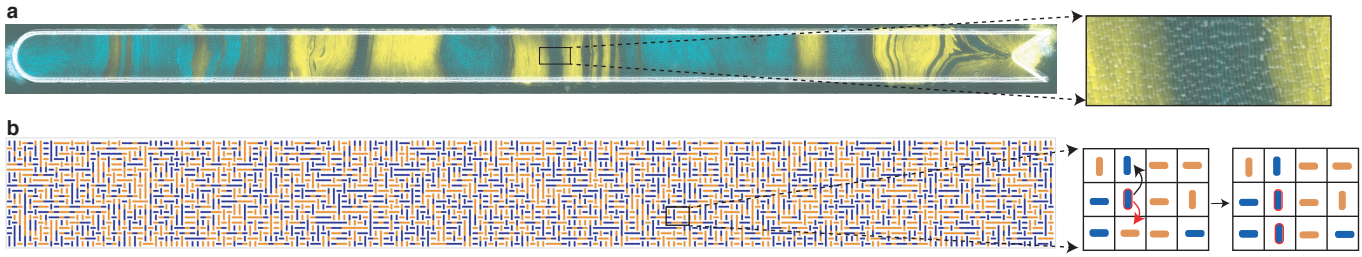

FIG. S1. (Color online) (a) Image of an extended microfluidic trap. The image in the main document is a zoomed in version of this trap. The enlargement on the right shows that cells align vertically so as to be orthogonal to the long boundary. (b) Another schematic of the SMM.

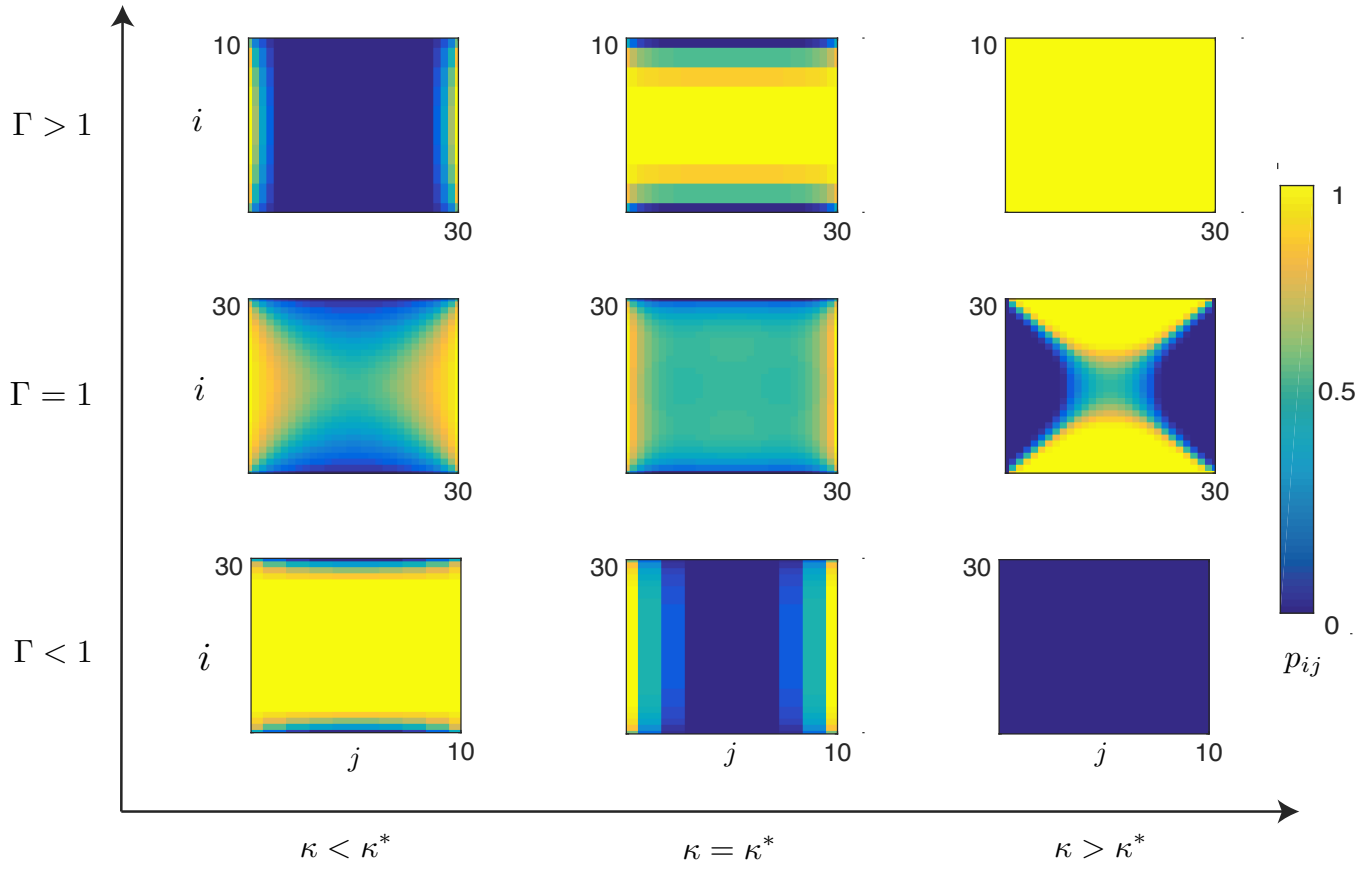

FIG. S2. (Color online) Steady states for Eq. (S2), the closed equation version of Eq. (2) of the main document for various values of κ and Γ. Here, $\kappa^* \approx 0.0072$. Note how for $\kappa < \kappa^*$, boundary layers emerge near the short boundary. These indicate a breakdown of the independence assumption, Eq. (S1). Other than this anomaly, Eq. (S2) captures the transition between steady-state cell alignments in microfluidic traps as shown in the original SMM.

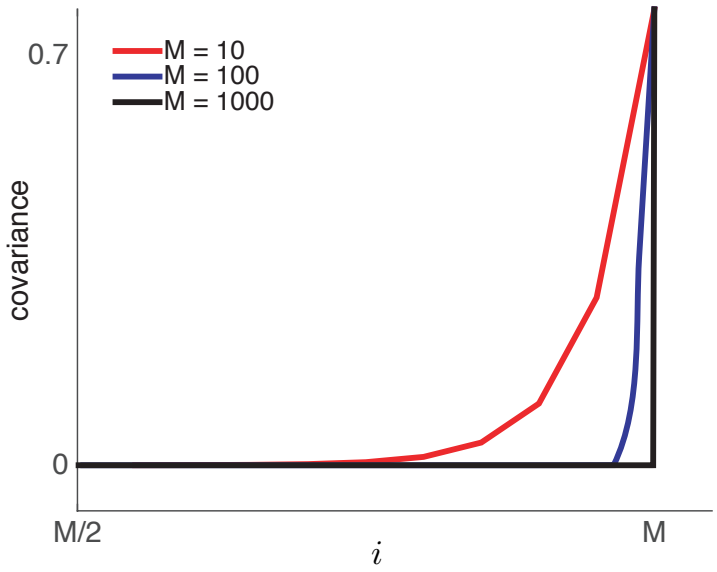

FIG. S3. (Color online) Plots showing how in the bulk of domain, covariances are close to 0, although in the $\kappa < \kappa^*$ case, covariances become more significant near the short boundary. All plots are for fixed $N = 7$. The curves are obtained from covariances of adjacent sites along the stripe $j = N/2$ from $i = M/2$ to $i = M$. As M grows, the decay of the covariance is more pronounced.

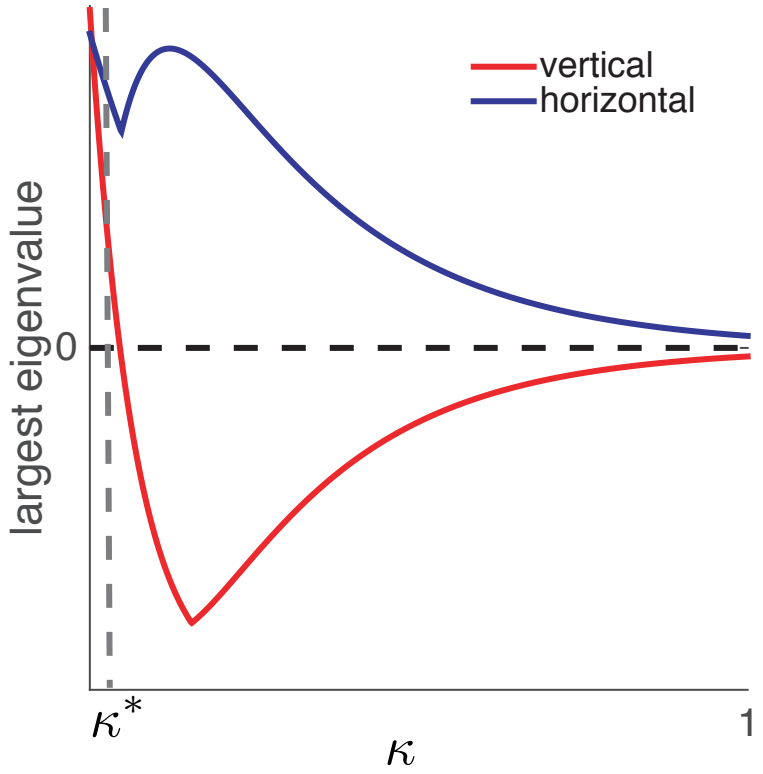

FIG. S4. (Color online) The real part of the largest eigenvalue of the Jacobian at $p_{ij} = 0, 1$ as a function of κ for $\Lambda > 1$ fixed. For most of $\kappa > \kappa^*$, the all-vertical state is stable. For some $\kappa > \kappa^*$ the vertical state is destabilized and a stable hybrid equilibrium emerges. In particular, the horizontal state never becomes stable. Hence, in the ME model of cell alignment, the κ-driven bifurcation is a transition between an all-vertical state and predominantly-horizontal state.

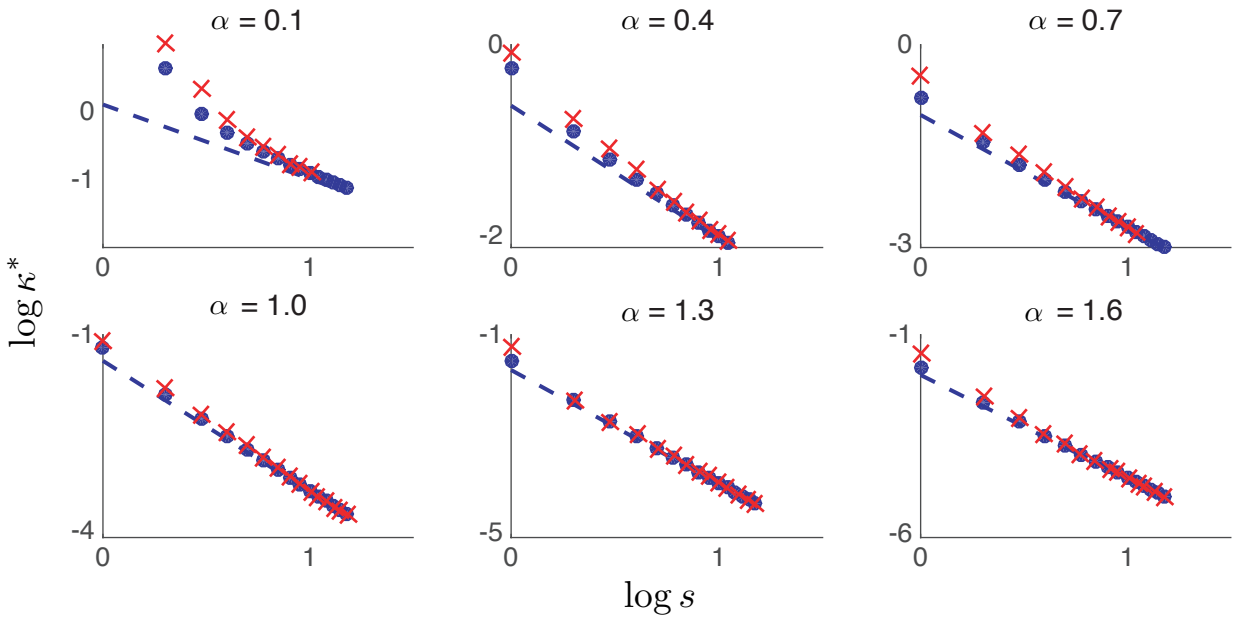

FIG. S5. (Color online) Plots of κ^* versus s for several values of α. For strong interaction kernels, theoretical asymptotic curves fit stochastic bisection values closely across a wide range. For weaker interaction kernels (see, for example $\alpha = 0.1$), for small trap sizes, s, the theoretically and numerically obtained values disagree. However, in all cases the theory correctly predicts the asymptotic behavior of the SMM. Crosses: κ^* obtained from the full stochastic model (SMM). Dots: κ^* obtained from growth rate of the mean field model. Dashed Line: Theoretical curve from asymptotics.

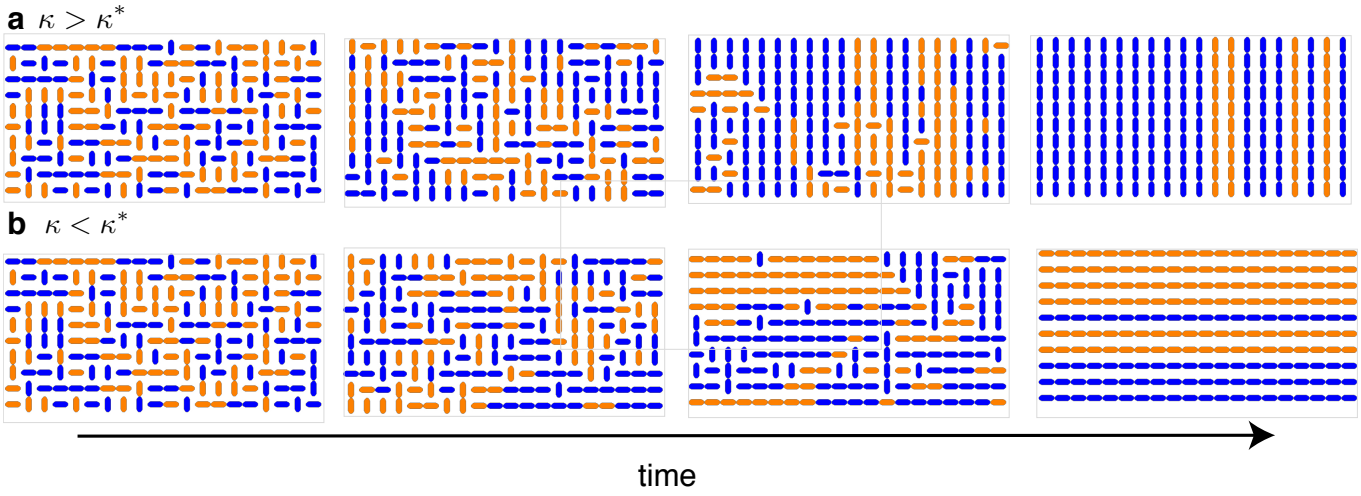

FIG. S6. (Color online) Cells growing on a lattice according to the long range model. (a) Time series for how system reaches equilibrium from the initial condition for $\kappa > \kappa^*$; (b) Same as (a) but for $\kappa < \kappa^*$. See online code for video depictions of this process. MATLAB and C++ code is available online for this model.